Modelling Guidelines for Thermo-Elastic Analyses

Alexander van Oostrum [(1)], Alberto Peman [(1)], Benoit Laine [(2)]

[(1)] ATG-Europe B.V., Huygensstraat 34 -2201 DK Noordwijk (ZH) -The Netherlands,
Email: alexander.vanoostrum@atg-europe.com / alberto.peman@atg-europe.com
[2)] European Space Agency, Keplerlaan 1, 2201AZ, Noordwijk (ZH), The Netherlands,
Email: benoit.laine@esa.int

KEYWORDS

Thermo-elastics, Interfaces, High precision, Prediction, Modelling, Guidelines

ABSTRACT

Increasing stability requirements and performance have resulted in Thermo-Elastic (TE) becoming ever more critical. Not only for high performance instruments, but also for their supporting structures. Currently, no guidelines exist in the ECSS for TE analysis. This paper provides a summary of an ESA funded activity looking into TE modelling methodologies and provides a first set of parameters that are important when modelling and analysing for TE.

For thermal models, an accurate representation of thermal gradient was found to be a key TE driver. Because of this, the thermal mapping method was found to be important, at least locally. For structural models it was found that models which behave similarly dynamically, can behave differently under TE loading, risking false confidence when these models are used for TE. In particular, the level of detail used in interfaces and sandwich panels (2D vs 3D) modelling showed significant effects.

1. INTRODUCTION

Forthcoming space missions require ever increasing levels of pointing accuracy. Due to these demanding requirements, it is of utmost importance to characterize and predict precisely the thermo-elastic behaviour of future spacecraft.

This paper provides a dissemination of the key observations and conclusions from an activity looking into TE modelling using a simplified version of the Euclid Service Module (SVM) structure. This study originated from the work performed by Thales Alenia Space Italy on the I-Meter study [1] which raised a number of questions that were not addressed in the original activity.

This work was funded by the European Space Agency, with the objective to complement the work performed in the I-Meter activity. A special thanks is extended to Thales Alenia Space Italy for allowing the models from the original study to be reused for this activity. In this context it is important to note that the model of the Euclid SVM structure represents a simplified version of the structure and has been adapted for the purpose of the activity. Hence, the results of this study will be representative for trends in such a typical configuration, but they do not represent the actual Euclid SVM structure.

The primary objective of this activity is to set first steps towards TE modelling guidelines through the investigation of modelling methods and TE processes. Given the very broad scope of the topic, this activity is too limited to provide definitive answers on how a generic structure should be modelled. Rather, for this specific model a non-exhaustive summary of key insights is provided. This summary may help the reader identify critical TE modelling aspects to be considered.

The work performed under this activity was split into two phases. The first phase focused primarily on the effects of thermal modelling and thermal mapping methods. Even for a structural analyst, these two topics are considered to be critical in a TE analysis, as a correct load definition is essential for an accurate prediction of the response. Therefore, the results presented in this study may help judge the quality of the thermal inputs and provide direction when applying the temperatures in the structural model. The second phase focused on structural modelling aspects, of which the influence of interface modelling and sandwich panel modelling will be discussed in more detail. Full details on both activities can be found in [2,3].

The structure of this paper reflects the two phases of the project. Between the two phases, model updates were applied to the configuration of the model. However, the key architectural features of the models have remained the same and are discussed in §2. Phase specific updates on the models, in addition to the results for each respective phase, can be found in §3 and §4.

2. MODELS

This section provides a comprehensive overview of the main architectural elements found in the models from both project phases.

The models, originally created by Thales Alenia Space, and re-used for this project, are based on a simplified version of Euclid SVM structure. Therefore, they may not fully represent the actual

Euclid SVM structure as they were originally developed for the specific purpose of the I-meter study and have been re-created for this study on TE modelling methods. They do however exhibit modelling aspects which may be found in real projects. The models are therefore considered representative, from a size, complexity, and modelling approaches, of typical spacecraft structures. This allows to complement some of the previous studies carried out by ATG [2,3,4], which were carried out on simpler and smaller models.

It is important to note, that the models in the second phase were updated with respect to the ones shown in this section. These updates are covered in §4. This section is intended to cover general characteristics and architectural features applicable to both models.

The simplified Euclid SVM model, outlined in Figure 1, can be subdivided into the following parts:

- 1 Top and 1 bottom sandwich panels (CFRP skins)
- 6 side sandwich panels (Al skins)
- 1 cone structure sandwich panel (CFRP skins)
- 8 shear sandwich panels (CFRP skins)
- 2 dissipative units (on the inside of side panels)
- 1 star tracker on the +Y –X corner (Al bar)

Core of sandwich panels is always aluminum honeycomb

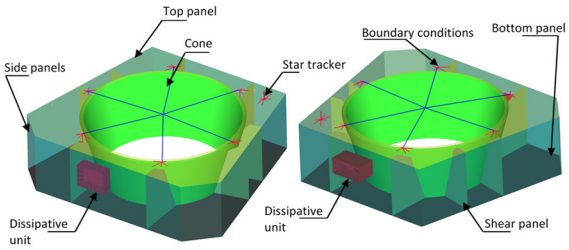

Figure 1: adapted Euclid SVM model overview representation

2.1. THERMAL MODEL DESCRIPTION

To perform the studies described in the following sections, different Geometric Mathematical Model (GMM) and Thermal Mathematical Model (TMM) were used. These models were rebuilt to allow for parametric meshing. Figure 2 displays the baseline geometrical mathematical model.

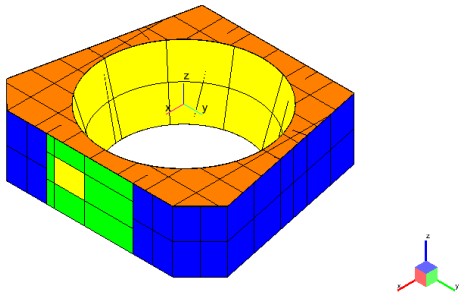

Figure 2: Baseline thermal model

The complete exterior of the thermal model is covered by Multi-Layer Insulation (MLI) except for the radiator (opposite to the dissipative units, in yellow on fig 2), payload interfaces, and star tracker locations. All the panels are modelled using two thermal nodes through the thickness: one thermal node for each facesheet.

The conductive links within each panel are computed using the automatic conductor generation option, part of ESATAN-TMS. The interfaces between the panels are implemented by automatically connecting the two closest thermal nodes (one on each panel) at each interface location with a representative junction GL.

The heat load on the phase 1 model was composed of a solar heat flux on the +Z top panel and 95W of heat dissipation by the internal units. Note, that these load cases are significantly different from the real Euclid SVM case. They were considered for the purpose of this study only. They should not affect the conclusions obtained from the study if they are applied consistently.
In phase 2 the solar heat flux was updated to hit on the +X panel and the position of the heat dissipating units were updated to the ±Y panels in order to make the model more representative of the real thermal environment.

2.2. STRUCTURAL MODEL DESCRIPTION

For both phases of the project a similar baseline model was used. The key mechanical features of these models are:

- 2D PCOMP Shell representation of the sandwich panels.
- Spring interfaces representing the brackets between the panels.
- RBE3 representing a point in space at the star tracker location.
- RBE2 + Point masses representing the dissipative units.
- RBE3 connecting the 6 attachment point of the SVM structure to the rest of the instrument (constraint is applied here).

It is acknowledged that this modelling approach is a simplification of reality. Especially the interfaces

may have a significant effect on the TE results.
As phase 1 of the project is focused on the "thermal" part of a TE analysis, this IF modelling should not affect the general trends in the thermal model and by extension the trend observed in the TE results.
In phase 2 these modelling simplifications become the point of attention. Specifically, the IF modelling methods and their effects are assessed in depth. In addition, the simplified modelling method of the sandwich panels is also investigated. Details on these models can be found in §4.

3. PHASE 1: THERMAL MODELING AND MAPPING METHODS

The investigations of phase 1 of this activity were mostly focused on the "thermal" step of the TE process. Two different aspects of this step and their effects on the TE results were looked at in conjunction:

- the effects of thermal model mesh refinement /convergence.
- the effects of different thermal mapping methods.

As such, both these aspects could be considered independent from each other, but the idea was also to investigate if there was any interaction between each other. Specifically, it was hypothesized how choosing an appropriate thermal mapping method might help with thermal model mesh convergence. This paper will consider a subset of the most interesting results. More results and conclusions for this study can be found in [2].

3.1. Thermal mapping methods

3.1.1. Methods used in this study

In the context of this paper the term "thermal mapping method" relates to the procedure on how temperature results are translated from lumped parameter thermal model (e.g. ESATAN-TMS) to Finite Element (FE) Model (e.g. Nastran). As part of this activity three thermal mapping methods were used:

- Patchwise method
- Conductive interpolation or Centre Point temperature (CPT)
- Prescribed Average Temperature (PAT) method, implemented through SINAS (see e.g. [5])

The methods can be characterized as follows:

The **Patchwise method** uses a direct correspondence between thermal nodes and FE elements. As such no interpolation of any form is needed. As a result, the temperature field will look very similar to the temperature field in the thermal model. Local variation in the temperature field due to, for instance, variations in the geometry or complex local features are, therefore, not considered unless the thermal model mesh is sufficiently refined to represent these. In Figure 3 the discontinuous temperature field can be clearly observed.

The second method is the **conductive interpolation** or CPT method. In CPT, thermal model nodes are not directly linked to all FE elements or GRIDs. Rather, the FE model is updated to include the same conductive properties as the thermal model. Temperatures for the thermal model nodes are then assigned to the GRID points which lie closest to the centre of these thermal node locations. A conductive FE analysis is then executed, using these selected GRID point temperatures as boundary conditions. Compared to the patchwise method this method has the advantage that it may be easier to implement (as only a selected number of GRID points need to have their temperature assigned) and it adheres better to local feature in geometry. At the same time, it may lose some of the intrinsic properties of the thermal model. Specifically, the average temperature of a thermal node over the area that it covers is not maintained. Figure 3 shows an example of the conductive interpolation.

Finally, the **PAT method** can be considered to be a combination of the above two methods. Similarly, to CPT, the FE model is updated to match the conductive properties of the thermal model. Using the PAT method an average temperature is prescribed to a group of elements, similar to the groups of elements in the patch wise method. Instead of applying the temperature on those elements directly, the conductive properties of the FE model are used to determine GRID point temperatures which are in line with the conductive properties of the FE model and which maintain the average temperature of thermal nodes. As such two of the key positive characteristics of the other two aforementioned methods are combined.

The effects that these three thermal mapping methods have on TE results were discussed in the previous edition of the ECSSMET [4]. Yet, the previous work focused more on the effects under idealized circumstances. This study provides a comparison on how these methods compare in a practical application.

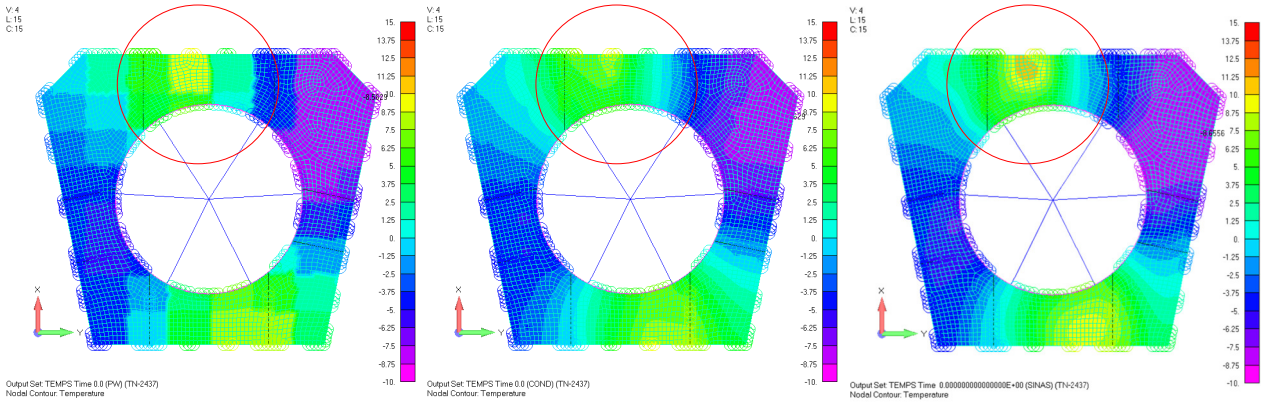

Figure 3: Temperature mapping methods comparison example. A: Patchwise method (left) B: CPT method (middle) C: PAT (SINAS) method (right). Region with most clear differences encircled

In the encircled region, where the temperature is driven by a radiative exchange with a nearby electronic unit located on the +X panel, clear differences between the methods can be observed. The patchwise method maintains the average temperature but creates a clearly unphysical discontinuous temperature field. Conductive interpolation does create a more realistic smooth temperature field but seem to underestimate the local temperature.
More far field, especially for conductive interpolation and PAT, the differences become much less apparent. The local peak temperatures in the PAT method are higher than those found in the thermal model. In general, these higher peak temperatures are found to be physical, as the nodes of thermal model represent the average temperature over a region. When peak temperatures are non-physical or happen at unexpected locations, they typically indicate modelling errors. More insight on the mapping method in conjunction with thermal mesh convergence is found in §3.2.

3.1.2. Other common methods not considered in this study

Two **other methods** which are commonly used in industry, but which were not used in this study are:

- Geometric interpolation
- FE Analysis

These methods were not considered for this study as they are very dependent on the exact implementation by the analyst, which may differ from case to case. However, as they are commonly used in industry, they are shortly recapped here such that the user of these methods can make a qualitative comparison for their own method.

Geometric interpolation method covers any form of temperature interpolation which does not use the conductive properties of the thermal model. Instead, the temperatures are determined using the weighted distance between GRID points and thermal nodes as interpolation functions. There is no exact definition of this method as the interpolation depends on the weighing factors selected or the exact interpolation functions. For simple geometries (plates etc.) these results may well be representative of the real temperature field. However, if locally there are very complex mechanical features, this may no longer be the case as this method cannot leverage the details of the more refined FE model in the same way that conductivity-based methods can [4].

Finally, in another commonly used method, the temperature results from the thermal model are not considered. Instead, a conductive FE model is used to perform the conductive analysis. Thermal loading (power dissipations in a purely conductive model) is directly applied. Such loading may be retrieved from a separate thermal model (e.g. external fluxes, radiative exchanges). This method has the potential to be equally or even more representative (for purely conductive problems) than a traditional lumped parameter thermal model. However, for more complex models, its accuracy will depend on how realistically the thermal loading can be applied such that the results match the thermal model results well. As such, this method was not considered for this study.

3.2. Thermal Mesh convergence

The second main aspect that was considered in this phase of the study was the level of thermal model refinement. For this purpose, thermal models with different levels of refinement were compared. In Figure 4 the different thermal models are shown.

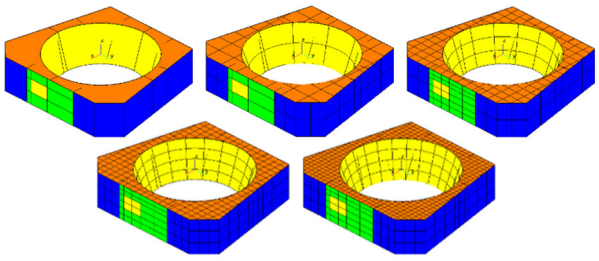

Figure 4: Thermal models at increasing levels of refinement

These models were refined differently in each region of the model. The refinement was performed per region to allow separate effects to be distinguished. For convergence, only global behaviour was subsequently assessed, no convergence criterion was used for the refinement of individual regions. For the -Z panel, not shown in Figure 4 a similar refinement to the one applied on +Z panel was used. For the back region, which houses the other dissipative unit and radiator, a higher refinement compared to the front panel was applied.

The thermal models themselves were not optimized to yield the highest accuracy for each given number of thermal nodes. When the primary heat paths are well understood and explicitly considered, it may very well be possible that better results can be achieved for an equal number of thermal nodes. An example of such a tailored mesh is shown in the second phase of this study, see Figure 10.

In Figure 5, the temperature results, on the FE model, are shown for the various thermal mapping methods as previously outlined in §3.1.1. Horizontally, the three thermal mapping methods are shown. Vertically, the five different levels of TMM refinement are shown, corresponding to the thermal models of Figure 4.

When comparing the results for the various models, clear variations in the temperature field can be observed. If the temperature fields and thermal mapping methods are considered three main conclusions can be drawn.

- There is significant temperature convergence in terms of thermal gradients within the panels (max-min temperature, per discretization). Especially for the coarsest thermal model, the discretization is obviously not sufficient.
- There is little temperature convergence in terms of average temperature of the panels. Although hard to directly see from Figure 5, the average temperature of all the panels is comparatively constant. For the +X and -X panel, housing the dissipative units, the average temperature varies less than 2.0 degrees. The other panels show slightly higher variance for the coarsest thermal model (<5.0 deg C), but also show an average temperature stable within 2.0 deg C for all other discretizations. This is considered an important metric for all models as the average temperature is an indication for the total distortive energy of each panel. In addition, the average temperatures may be an indication whether temperature uncertainty margins (which are often of similar order of magnitude or higher e.g. ±5 deg C) are sufficient to cover these kinds of phenomena. What seems to be more important for these models are the peak temperatures for each panel.
- Clear local differences in the temperature fields between the various thermal mapping methods can be observed. This is in line with the conclusions and observations from §3.1 noting that, specifically, the PAT method appears to improve local temperature field convergence. However, for the coarse discretization the PAT method creates unphysical temperature fields. In this model this can be observed by “cold spots” around the radiator (bottom right sub-figure of Figure 5). From experience, this unphysical behaviour can be leveraged as it typically indicates either a modelling error or a thermal model mesh that is not sufficiently converged, thereby giving useful hints were a model should be improved.

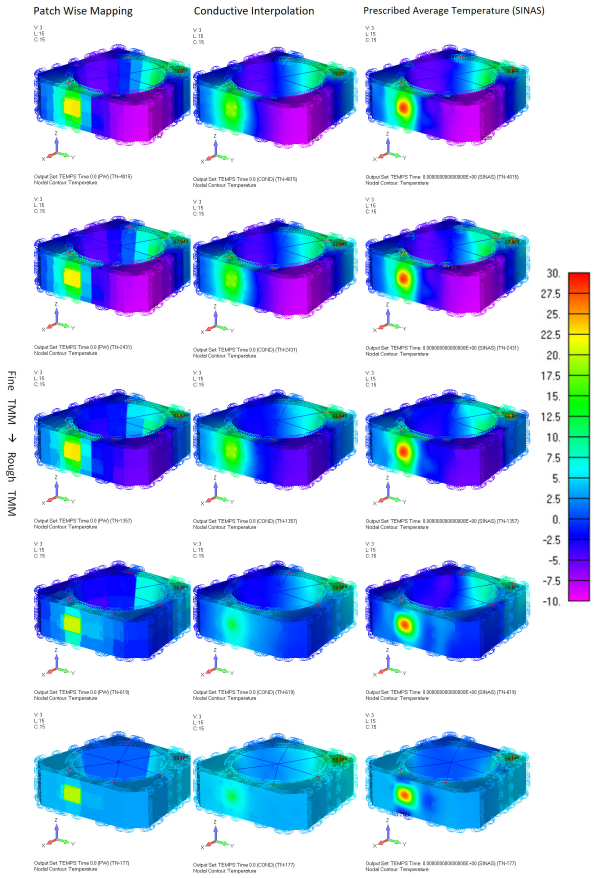

Figure 5: Temperature mapping and thermal mesh convergence result comparison

3.3. TE Results of combined effects

Using the different temperature field cases shown in Figure 5, various TE analyses were performed on the model and their results compared. An extensive set of results was processed and analysed. Here a short summary is provided for the most striking results. The results can be grouped into two categories: far field result and local results.

3.3.1.Far field results

In Figure 6 and Figure 7 interface force results are shown for two locations far away from the dissipative units. These examples show a particularly large and clear variation. Similar trends can be found in many other locations throughout the model. The exact position of these interfaces is hence not very relevant. The key observations here would be:

- The effect of thermal model mesh convergence has a significant impact on the results.
- Even though the average temperatures (distortive energy) in the panels is rather stable, the results at the interfaces are not; further amplifying the importance of the thermal gradients.
- The differences between thermal mapping methods are small, and are insignificant compared to the effects of thermal model mesh convergence.

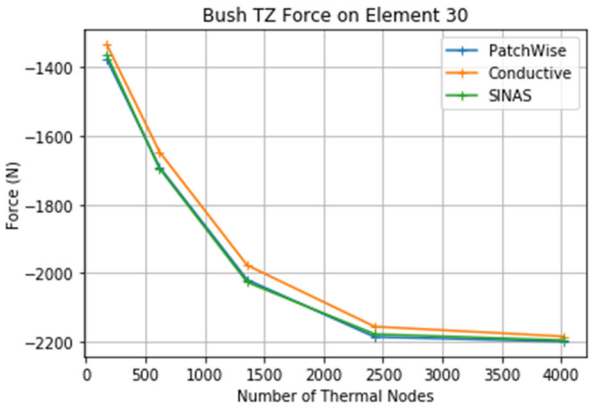

Figure 6: Example force results for a location far field from the source of the dissipative units

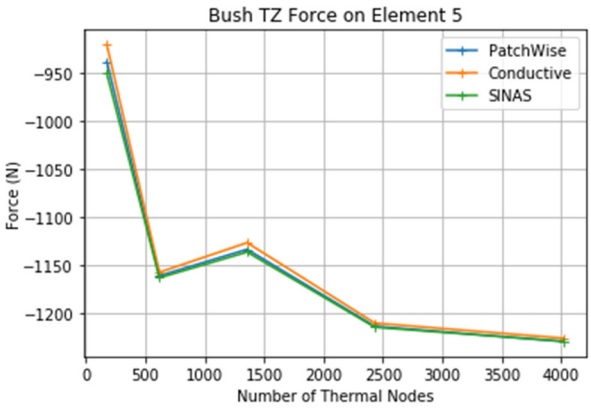

Figure 7: Example force results for a location far field from the source of the dissipative units

The importance of the thermal gradients is considered the **key observation** from this study. What remains an open question is whether the large variations in the results follow directly from the increase in temperature gradients or, are indirectly due to an amplifying effect of the Coefficient of Thermal Expansion (CTE) mismatches between the panels. Regardless, the importance of temperature gradients, for this model at least, is clearly demonstrated.

3.3.2. Local results

When the local results are considered, the regions around the dissipative units are interesting. Around these regions, the effect of the thermal mapping methods also becomes apparent. One of these regions was already shown in Figure 3 for purely thermal effects. In Figure 8, the results for an interface close to the dissipative unit are shown.

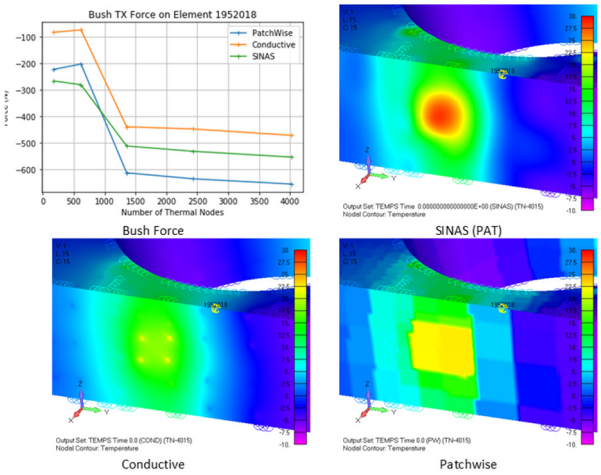

Figure 8: Example force results for a location close to the dissipative units

From the results, it is clear that, locally, the temperature mapping methods have a significant impact. Particularly, it can be noted that the CPT method is not able to handle regions with high dissipations well. Still, also in these more local regions, the thermal model mesh converge effect is considered driving [2]. This is as expected. If a thermal model mesh has not converged globally, then, the interpolation methods will not help the thermal model mesh convergence, as they cannot add this information. The results for the –X panel, where the thermal model mesh was more refined, provide a similar picture.

At the start of this activity, it was assumed that certain temperature mapping methods might help with convergence of the temperature field, without needing to refine the thermal model. While this theory is not proved invalid - actually locally improved temperature convergence was observed for the PAT method [4] - it is clear that for this particular model, the mapping method is not the dominant contributor to the results. For this model, the global thermal model mesh convergence is more important. A factor which was previously considered to be the key conclusion of this phase. This key conclusion does not invalidate the original hypothesis. It is likely that for problems with more well-defined conductive heat paths (e.g. through an instrument, flexures etc.) and less radiative effects, this could still be the case, and would be in line with the original hypothesis. For this specific model, the

thermal mesh is still considered to be rather coarse and would need to be refined further to really see if this would apply to this model.

4. PHASE 2: STRUCTURAL MODELLING

The investigations of phase 2 of this activity were mostly focused on the "structural" part of the TE process. Two aspects were looked at independently. To study these aspects, some changes were introduced into the baseline models. The new baseline thermal and structural models were modified to consider the conclusions from the first phase of the project. Figure 9 shows the baseline model, highlighting a detailed section which is investigated as part of this study. All analyses are still performed on the full model, but updates as part of the sensitivity studies of this phase only consider the detailed section. In Figure 10 the new thermal model is shown. Results and details on the new thermal model are not repeated, and focus is laid on the structural model in this phase. The applied changes are described in detail in [3].

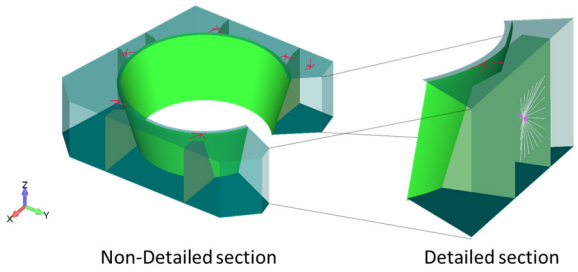

Figure 9: Phase 2 structural model

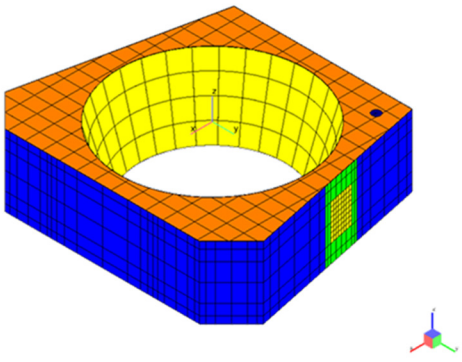

Figure 10: Phase 2 thermal model

In the European space community, various ways of modelling interfaces (IFs) in FE are used. In most cases, no matter which IF modelling method is used, the IFs' stiffness can be tuned such that the main dynamic modes of the structure, in the FE analyses, match the dynamic test results. Nevertheless, these different IF modelling methods do not always have the same thermo-elastic properties due to their inherent formulation. Therefore, the first question to answer in the second phase of the project was: *do different IF modelling methods with similar dynamic behaviour also display similar thermo-elastic behaviour?*

On a similar topic, within the FE field there are several ways of modelling sandwich panels. Even when applying large simplifications to a sandwich panel model the dynamic behaviour can be captured well. Therefore, similarly to the first question in this phase: *do different sandwich panel modelling methods with similar dynamic behaviour also display similar thermo-elastic behaviour?*

The second phase of the activity also covered the impact of:

- The modelling detail of substructures on the TE results.
- the inclusion of through thickness temperature gradients on TE results.

The results and conclusions to these other sub-studies can be found in [3] and are not further discussed as part of this paper.

4.1. TE behaviour comparison as a function of the IF modelling approach.

To answer this question, the bracket IFs between the panels, in an area of interest of the structural model, were modelled using three common industry approaches. In this case, the area of interest studied was the area surrounding the dissipative unit on the +Y panel. The 3 different modelling methods (see also Figure 12) used at this location to represent the brackets were:

a. 3 Spring elements (baseline case)
b. 1 Spring + 2 RBEs (rigid)
c. 6 Springs + 12 RBEs (rigid) + bracket model

In order to later be able to compare the IF forces between the three modelling levels, the forces of the spring elements for each case were combined as shown in Figure 12. In total there were 39 brackets in the detailed section.

A dynamic "correlation" was carried out between the two new FE models and the baseline case to match the main dynamic response of the models. As the first resonant frequency of the +Y panel describes the main dynamic behaviour of the detailed section being studied, only that frequency was matched (80.4Hz). Figure 11 shows the shape of the main mode for the +Y panel.

shape of the +Y panel

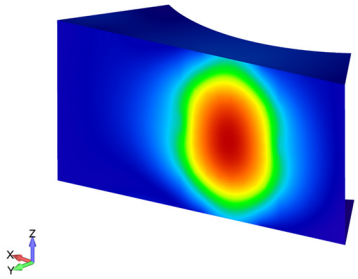

Figure 11 1st resonance frequency (80.4Hz) mode

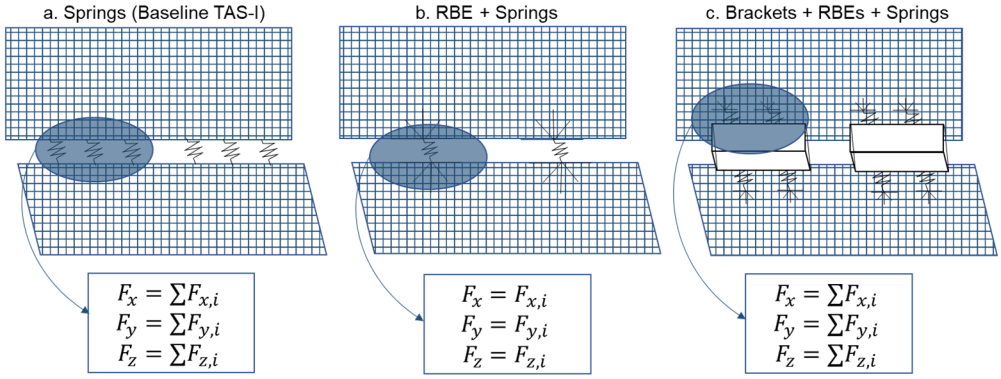

Figure 12: Types of interface links studied in Phase 2 (schematic representation)

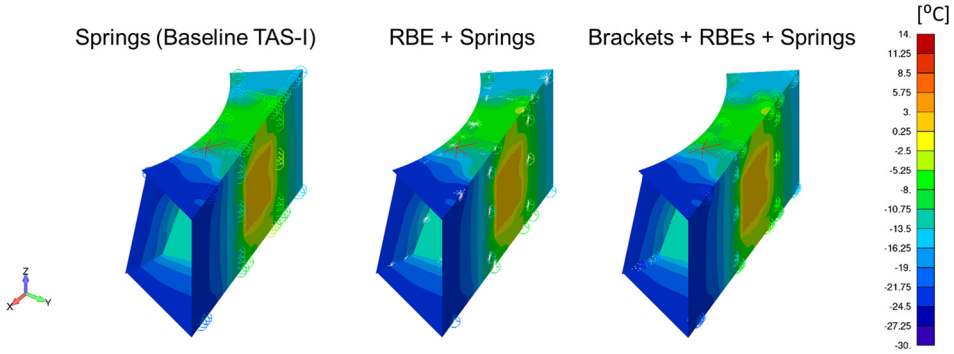

Figure 13: Mapped temperatures for the three IF cases. Only the detailed area of the model is shown

This correlation approach was deemed sufficient for the purpose of this study as the +Y panel is the only area where modifications were introduced, and generally, dynamic correlations are only performed using the main resonant frequencies. The correlation was performed by tuning the stiffness of the springs in the two new models until the main modal frequency of the +Y panel came within 1Hz of the frequency in the baseline case.

During the study, it was found that the dynamic response could be matched by modifying the spring's stiffness in several ways. For example, the "correlation" was achieved both by modifying the stiffness only in a specific direction and by modifying the springs' stiffness by a different factor but in all directions at the same time. It was also found that the case **c** model's IFs could be dynamically matched to the baseline case if the rotational spring stiffnesses were set to 0 (krot=0). It is important to note that this paper only shows the results when a single spring stiffness direction is tuned, for further information please refer to [3].

The "correlation" results are summarised in Table 1. The results show that even though the modelling method for the IFs was changed, the dynamic behaviour of the new models could be matched to the one shown by the baseline case within an acceptable degree of accuracy (less than 1% difference).

Table 1: Dynamic response correlation results when spring stiffness in all directions is modified.

IF modelling Case	**Tuned Freq [Hz]**
a. Spring elements (baseline case)	80.4
b. Spring + RBE	80.4
c. Spring + RBE + bracket model (krot = 0)	80.0
c. Spring + RBE + bracket model (krot ≠ 0)	80.2

After matching the dynamic behaviour of the 4 models, the temperature field from the thermal

model was mapped onto the structural FEM using the PAT (SINAS) method (see §3.1.1) and a static analysis was run. Figure 13 shows the mapped temperatures on the FE model for all 3 IF cases.

Once the TE analysis was computed, the forces for each IF were extracted and compared to the baseline case. Eq. 1 displays the IF force ratio with respect to the baseline. The IF force was computed per fixation point as per Fig. 12.

$$\Delta F = \frac{F_i}{F_{baseline}} \qquad (1)$$

As shown in Fig. 14, global differences in the TE joint forces are observed between the different types of joint models for these specific models. For some interfaces these may be of the order of 60% different. These differences appear to have no particular trend in the IF's location or method of tuning the dynamic behaviour. It is also interesting to notice that the results show differences larger than the conventional Km modelling factor 1.2. Although not shown, similar results are seen when the IF stiffness is tuned in all directions [3].

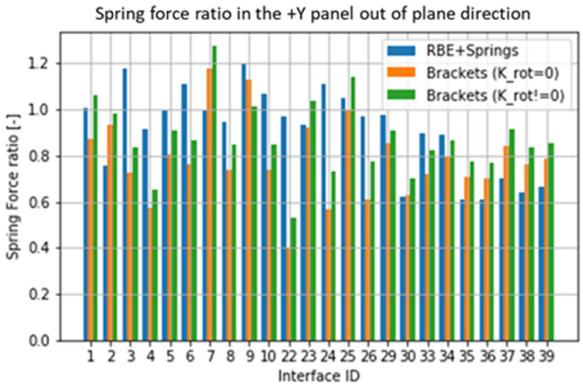

Fig. 14*: IF force ratio of the different correlated cases with respect to the baseline case. (IF with loads<100N were removed from the plot)*

The rotation fields in the different cases were also extracted and compared. Figure 15 shows the rotation field of the model case a. (baseline) around the X axis.

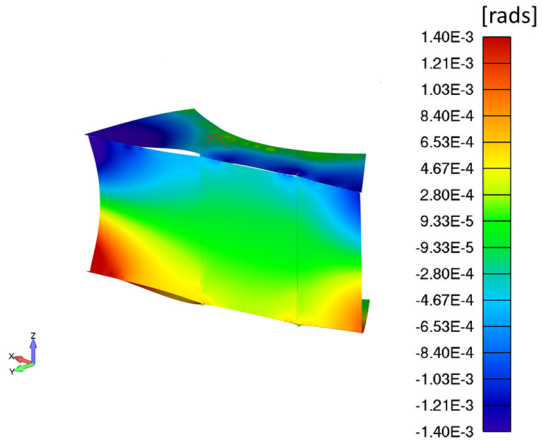

Figure 15: Rotation field around X axis on the Case a. model (baseline)

The rotation fields for the model cases b. and c. were also extracted and their difference with respect to the baseline case is shown in Figure 16. These plots show a global distribution of differences of up to 30%.

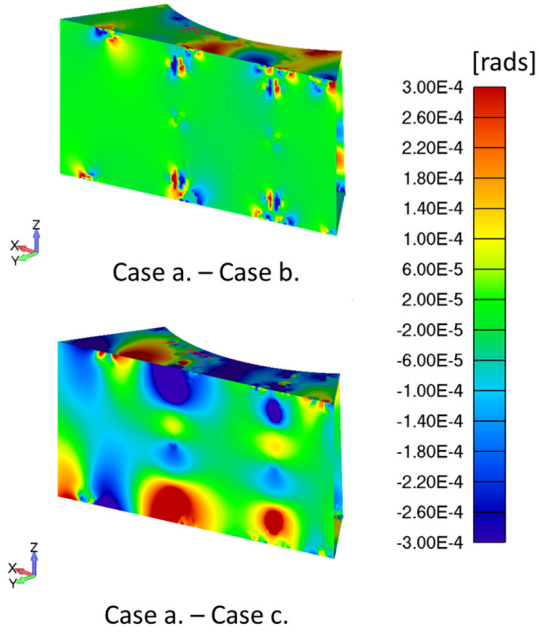

Figure 16: Difference in rotation around the X axis of Cases b. and c. with respect to the baseline model

Effects from the different TE behaviours between joint models can also be seen far-field, at the star tracker location. Difference in variation of the star tracker Line of Sight of up to 19% can be seen for this case.

These results suggest that, in this case, TE analyses have in general a higher sensitivity to the joint modelling than dynamic analysis. It still needs to be assessed if these differences in the results are caused by the intrinsic mathematical differences regarding TE behaviour between the IF model types, or, if the stiffness range is narrower when

correlating TE results than when correlating dynamic responses. Yet, it is clear, that care should be taken if a simplification to the IFs in models is going to be made and that a simple dynamic comparison may not be conclusive.

These results are unsurprising, considering that the dynamics are likely mostly driven by the out-of-plane stiffnesses, whereas for TE in-plane stiffness are likely more important.

It should be noted here that within this activity an originally coarse and simplified model was updated to account for increasing level of detail. This is considered to be a less than ideal approach, especially since exact bracket details (on which the stiffness of the original spring might have been based) were not known. If this exercise was performed in reverse, going from a refined to coarse model, then the results may have been somewhat less striking. Still, that does not invalidate the results that a seemingly similar dynamic model – that may even be correlated after a test – may behave quite differently under TE loading. More so, the fact that similar results could be obtained by updating the spring stiffnesses, implies that the compliance of the bracket had at best a small contribution to the overall joint stiffness only.

As such, care should always be taken when simplified models are used, and "typical" stiffness values, which may be representative for dynamics, can be very unrepresentative for TE predictions.

4.2. TE behaviour comparison as a function of the sandwich panel modelling approach.

To answer the second question, the 2D plates +Y panel (panel a.), in the FE model with the model with highest level of detail (i.e. with brackets) from the previous task, was substituted by a detailed 3D solids element panel (panel b.). By comparing the TE results on both panels we could assess the differences in TE behaviour between a 3D sandwich panel and a 2D plate panel.

The new model (containing panel b) was fully built using PLATE elements with PCOMP properties except for the +Y panel. The +Y honeycomb panel was modelled using PLATE elements for the facesheets (homogeneous aluminium properties) and SOLID elements for the core (MAT9 card used for the core with aluminium honeycomb properties). At the connection points in the +Y panel, the panel properties were swapped for Al and Ti insert properties (both cases were studied, and no major differences were observed in the results). The inserts were modelled all the way through the thickness at structural connection points and halfway through the thickness at unit mounting points.

In order to keep the stiffness of both panels the same, the properties of the new 3D panel were selected to match the out of plane and in plane stiffnesses of the 2D panel. Unitary displacement load cases were computed to verify the equivalence of the panel's stiffness. In this case, the CBUSH stiffness was not changed even if the dynamic behaviour was slightly modified (less than 1.5Hz) in order to keep the conclusions independent of a possible IF stiffness change. The new 3D +Y panel is shown in Figure 17.

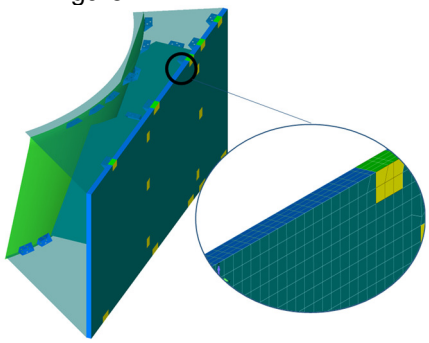

*Figure 17: Detailed view of the new FE model containing panel **b***

The temperature field from the thermal case was then mapped onto both models using the PAT (SINAS) method and taking the through thickness temperature gradients into account for both models. An FE temperature plot is shown in Figure 18 comparing the detailed section for both models. It can be observed that the temperature loads in both models are very similar. After performing each temperature map a static TE analysis was performed on both models. A different load case, with average through thickness temperatures was also studied but is not shown in this paper, for further detail refer to [3].

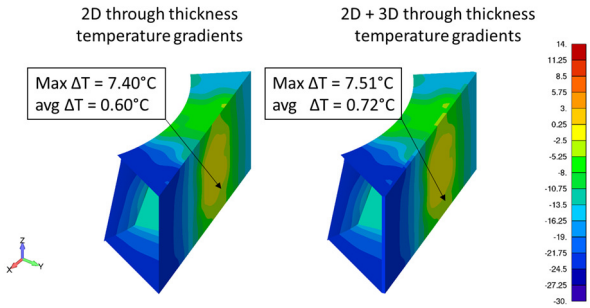

*Figure 18 Detailed view of the temperature fields in both FE models. Labels indicate the maximum and average through the thickness temperature gradients in both panels **a** and **b**.*

For each IF, the forces in every direction were computed and compared. Figure 19 displays the ratio (panel b./ panel a.) between the IF forces in each panel with through thickness temperature load case. The force ratio shown refers to the forces in the out of plane direction of the panel. These results show how even though the stiffness, dynamic behaviour and temperature load of the 3D panel is almost identical to the 2D panel, the TE behaviour shows significant differences at the joint forces for these models.

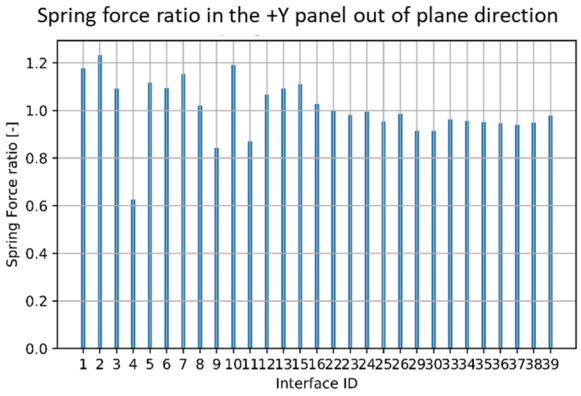

Figure 19: IF force ratio of the between panel b. and panel a. *(IF with loads<100N were removed from the plot)*

The IF forces were computed keeping the stiffness of the IFs equal to the 2D case. The main resonance frequency for the panel showed little variance but the thermo-elastic results showed a difference in IF forces larger than 20% in several locations. These differences were mainly caused by the change in detailing level of the +Y panel.
Therefore, this study showed that, for this model, 3D modelling of a sandwich panel induces significant variations in local joint forces and rotations fields compared to a more simplified 2D shell model of a sandwich panel.

In addition, in the full study [3], It was found that it was easier to apply through thickness temperature gradients on a 3D panel than on a 2D panel. For this model, it was found that these gradients can have significant contribution to the local results (differences of up to ~20% for this model).

5. CONCLUSIONS

In this paper the key results of two phases of an ESA funded activity into methodologies for TE modelling and analysis were described, providing useful insights into the importance of the modelling approaches on TE results. Using a simplified version of the Euclid SVM, several aspects in thermal modelling, structural modelling and thermal mapping methods were investigated.

The results of these activities can be considered as an extended sensitivity study. The models provide a useful additional degree of complexity and representativeness compared to previous work (e.g [4]) that considered very simple examples such as plates. Therefore, the results should provide insights into important factors to consider.

Nevertheless, there are many different types of models, configuration and structures which may all be driven by different factors. Main drivers to consider in this regard are CTE (mismatches), how a model is constrained (internal load paths), the absolute temperature levels and the thermal gradients. Some of these considerations may turn out to be leading for certain kinds of structures whereas they may be less relevant for others.

For this activity, the studied model had significant temperature gradients and temperature averages close to the material reference temperature (20 deg C). In addition, this structure featured many complex interfaces, which created hyperstatic constraints between the panels. Furthermore, some of these panels featured CTE mismatch with the adjacent panels (Top/Bottom panels vs lateral panels).

Taking these considerations into account, for the separate phases, the following can be concluded. For phase 1, the effects of thermal model mesh convergence and the thermal mapping method were investigated. It was concluded that:

- Thermal gradients are a key driver for the TE result of this structure. The results showed that even for models with a rather similar average temperature, significant variations between the results can be obtained when the thermal mesh is refined to better capture thermal gradients. These variations could be found throughout the whole structure. For highly loaded interfaces, variations of +60% at the interface forces could be noted.
- The thermal mapping method that is used has a lower impact for this structure than the effect of the aforementioned thermal gradients. Only locally, the temperature mapping methods appears to have an effect. For these local regions, none of the mapping methods provided consistently conservative (IF Force) results.
  Furthermore, the assumption that a thermal mapping method could aid thermal model mesh convergence could not be proven for this specific structure. Yet, locally, the PAT method provides more realistic thermal gradient. Still, the TE effects were for this structure dominated by the effect of convergence in the temperature field of the thermal model.

For phase 2, the effects of structural modelling were investigated. It was concluded that:

- The same model with different interface modelling methods, exhibiting a similar dynamic behaviour, may behave very differently thermo-elastically. This study showed up to 30% difference in rotation fields and up to 60% difference in IF forces. It demonstrates that TE prediction is very sensitive to local stiffness modelling, much more than dynamic results. This in itself is not a surprising conclusion and in much simpler structures it is intuitively obvious. Still its impact is significant. Often, models used for dynamics are also used for TE.

The fact that such a model is dynamically correlated may give a false sense of confidence that it may also represent the stiffness in TE problems when in reality it does not. Further research needs to be performed in order to determine best modelling practices.

- The second main observation of this phase was that the modelling method of sandwich panels (2D composite shells vs a full 3D model) also appears to have a significant impact on TE results. In this project differences of up to 40% in IF forces were captured even though both models showed a similar dynamic behaviour. Therefore, this again appears to be an issue that has little impact on the static/dynamic behaviour but a more significant impact on the TE response.
  In addition, locally, the effect of through thickness temperature gradients in the model were found to have significant contribution. Therefore, considering the practical difficulties of effectively applying temperature gradient to 2D shell models and the general discrepancies found between 2D and 3D models, a 3D model might prove to be most versatile.

All in all, this means that simplifications, removing detail from the dynamic model to keep their size manageable, may not be justifiable for a TE model. The study shows that great care has to be taken on the modelling used for TE analyses. When possible, a sensitivity analysis on mesh density and different ways of modelling is advisable, to get an idea of the possible uncertainties due to modelling assumptions. In all cases studied, the effect of modelling assumptions is greater than the typical model factor of 1.2.

For future work it is recommended to look into more different types of structures, all with realistic and complex models, where possible amended with test data. For now, when extrapolating these conclusions to different kind of structures, care should be taken and the key TE drivers and the general TE criticality of a structure should be assessed separately. Even though these models, in this study, were coarse and simplified, they provide useful insight and attention points when creating a model for TE analysis.

6. REFERENCES

1. Perachino L., Laine B., De Palo S., Mareschi V., Acquaviva F., D'Amico J., Behar-Lafenetre S., Baussart Ph., Appel S., Vaughan M., Sablerolle S., Ertel H., De Cillia M., Atinsounon P. (2021) Methodologies for thermoelastic predictions and verification. European Conference on Spacecraft Structures, Materials and Environmental Testing.

2. Alexander Van Oostrum, A., Peman, A. (2020). Investigations into Methodologies for Thermo-Elastic Predictions by Analysis. *ATG-RP-0013-19 iss.1.*

3. Alexander Van Oostrum, A., Peman, A. (2020). Investigations into Methodologies for Thermo-Elastic Predictions by Analysis – phase 2 (structural modelling focus)

4. ATG-Europe B.V., (30 May 2018)., ECSSMET, Temperature Mapping for Structural Thermo-Elastic Analyses: Method Benchmarking.

5. ESA, Introduction to SINAS (07-02-2012) *https://exchange.esa.int/download/sinas/TEC-MTV_SINAS_2012-02-07.pdf*